Current Optics and Photonics
Vol. 5, No. 2, April 2021, pp. 134–140

ISSN: 2508-7266(Print) / ISSN: 2508-7274(Online)
DOI: https://doi.org/10.3807/COPP.2021.5.2.134

Broadband Phase-change Metagrating Design for Efficient Active Reflection Steering

Sun-Je Kim*

Department of Physics, Myongji University, Yongin 17058, Korea

(Received January 25, 2021 : revised February 20, 2021 : accepted February 24, 2021)

In this paper, I introduce a novel design method of a high performance nanophotonic beam deflector providing broadband operation, large active tunability, and signal efficiency, simultaneously. By combining thermo-optically tunable vanadium dioxide nano-ridges and a metallic mirror, reconfigurable local optical phase of reflected diffraction beams can be engineered in a desired manner over broad bandwidth. The active metagrating deflectors are systematically designed for tunable deflection of reflection beams according to the thermal phase-change of vanadium dioxide nano-ridges. Moreover, by multiplexing the phase-change supercells, a robust design of actively tunable beam splitter is also verified numerically. It is expected that the proposed intuitive and simple design method would contribute to development of next-generation optical interconnects and spatial light modulators with high performances. The author also envisions that this study would be fruitful for modern holographic displays and three-dimensional depth sensing technologies.

Keywords : Grating, Diffraction, Metasurface, Subwavelength structures, Spatial light modulator
OCIS codes : (050.1950) Diffraction gratings; (050.6624) Subwavelength structures; (230.6120) Spatial light modulators; (230.7400) Waveguides, slab; (240.5440) Polarization-selective devices

I. INTRODUCTION

Over the past decade, rapid advances have been achieved in developing high-performance flat optic elements based on metamaterials and metasurfaces providing revolutionary improvement of optical functionalities, form factor, and integration density, beyond the classical refractive and diffractive optic elements [1]. Among various working principles, optical gradient metasurfaces capable of imparting local phase change and extending Snell's law of refraction and reflection [2], have risen as the most powerful and effective design principle to manipulate scattered optical wavefront in extraordinary manners. As a result, various flat meta-optical elements steering free space beams have been successfully demonstrated by exploiting dielectric or metallic nanoantenna designs for beam deflection, lensing, and hologram [3–9]. Modulation of free space beam direction is the fundamental functionality in optical information processing systems including interferometer, optical interconnect, optical data storage, and holographic displays [10].

However, most of optical metasurfaces made of dielectric or metal only provide fixed functionalities once they are designed and fabricated. Active optical metasurfaces can tune scattering properties in desired ways according to applied external stimuli [11] so that they would play pivotal roles in a wide range of optical imaging, display, and sensing applications. Among many active optical platforms, phase-change materials (PCMs) such as vanadium dioxide (VO_2) [12–17] or chalcogenide compounds [18–21] have attracted much attention in the nanophotonics community for the use in demonstration of actively tunable metasurfaces owing to their excellent tunability in optical frequencies. By virtue of such advantage and the following large design degree of freedom of nanostructures, PCM would be the

*Corresponding author: sunjekim@mju.ac.kr, ORCID 0000-0002-9627-4465
Color versions of one or more of the figures in this paper are available online.

most powerful material candidate in the visible and near-infrared regime, when compared to other platforms such as transparent conducting oxide and graphene [22, 23]. It is worth noting that VO_2 shows the giant insulator-to-metal transition (IMT) at the relatively low critical temperature (~68 °C) [24]. Based on the IMT, many researchers have reported active beam steering metasurface devices based on gap plasmons [21, 25] or Mie resonances [26]. Yet, these principles combining strong subwavelength resonances and generalized Snell's law of reflection are not able to meet on-demand multi-objective performances with broad operation bandwidth, high signal efficiency, and large extinction ratio, required for practical applications.

In 2018, my colleagues and I demonstrated a high performance active diffractive metagrating that consists of dual VO_2 ridge waveguides (VRWs) working in the optical communications regime [14]. The proposed mechanism based on weakly resonant waveguiding and transverse electric (TE) polarization enables high diffraction efficiency without plasmonic loss and severe chromatic dispersion.

Based on the previous study, here, I propose a novel multi-objective design method of flat high-performance beam deflector exploiting active VRW arrays combined with a metallic mirror. To simultaneously achieve broad bandwidth, enhanced optical efficiency, near-unity modulation depth, the VRW metagrating is designed and verified via theoretical calculations and numerical simulations. Compared to the inverse design and topology optimized devices based on brute force numerical optimization algorithms [27], the proposed design rules provide more simple geometry with physical intuition, relieved fabrication feasibility, tolerance, and cost, ease of design improvement, and potential combination with electro-thermal electrodes to the substrate mirror without sacrificing optical design performance.

The rest parts of the paper are as follows: first, the basic concepts are introduced. Then, numerical design processes and results of modulation performances of tunable beam deflectors and a tunable beam splitter are presented. Last, the conclusion is presented with summary and future perspective. In this study, numerical electromagnetic simulations are conducted by the conventional rigorous coupled wave analysis [28] and permittivity data of aluminum is quoted from [29].

II. RESULTS

Figure 1(a) shows ellipsometry result from our previous work [14] of largely switchable optical permittivity spectra of VO_2 grown on a sapphire substrate by pulsed laser deposition. It is remarkable that in the near-infrared regime, the real part of VO_2 permittivity changes its sign according to the phase. In the metallic phase, VO_2 acts as a plasmonic metal while the insulating VO_2 is a lossy dielectric with high index. It implies that TE polarized light cannot penetrate into the hot metallic VO_2 and can be guided in the cold

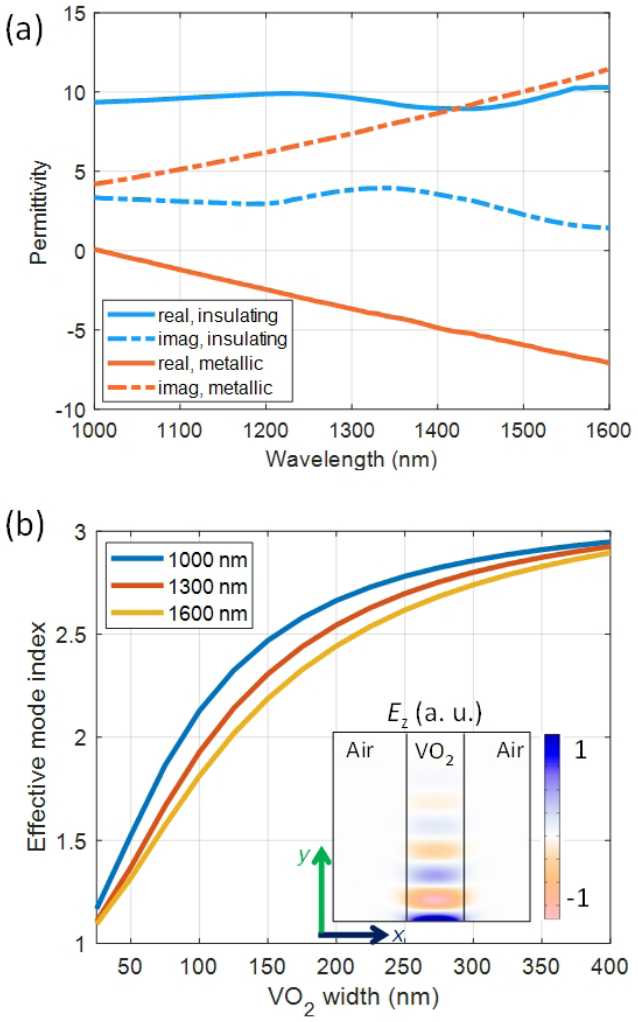

FIG. 1. Optical dispersion of VO_2. (a) Optical permittivity spectra of VO_2 at the insulating and metallic phases. (b) Effective fundamental mode index of one-dimensional VO_2 slab waveguide at the wavelength of 1000 nm, 1300 nm, 1600 nm, according to the varying slab width. The inset figure shows transverse electric field profile when the width and wavelength are 400 nm and 1000 nm, respectively, and VO_2 is at the insulating phase.

insulating VO_2 waveguide as shown in Fig. 1(b). The plot shows the fundamental TE mode of the VO_2 slab waveguide in the air depending on the width of the VO_2 slab, when VO_2 is at the insulating phase. Leveraging this largely switchable characteristic of VO_2 waveguide, penetration of TE polarized light into the waveguide structures and optical phase shift from the structures can be engineered.

Figure 2(a) shows the concept illustration of the supercell structure of the proposed active beam steering device with thermally switchable deflection angle over broad bandwidth. I utilize an aluminum mirror as a substrate for efficient operation, and VRW structures are arranged with varying width and fixed thickness of 200 nm on the mirror. The supercell period (4Λ) is set to yield only three diffraction orders (-1^{st}, 0^{th}, and 1^{st}) in the reflection side. Then, the

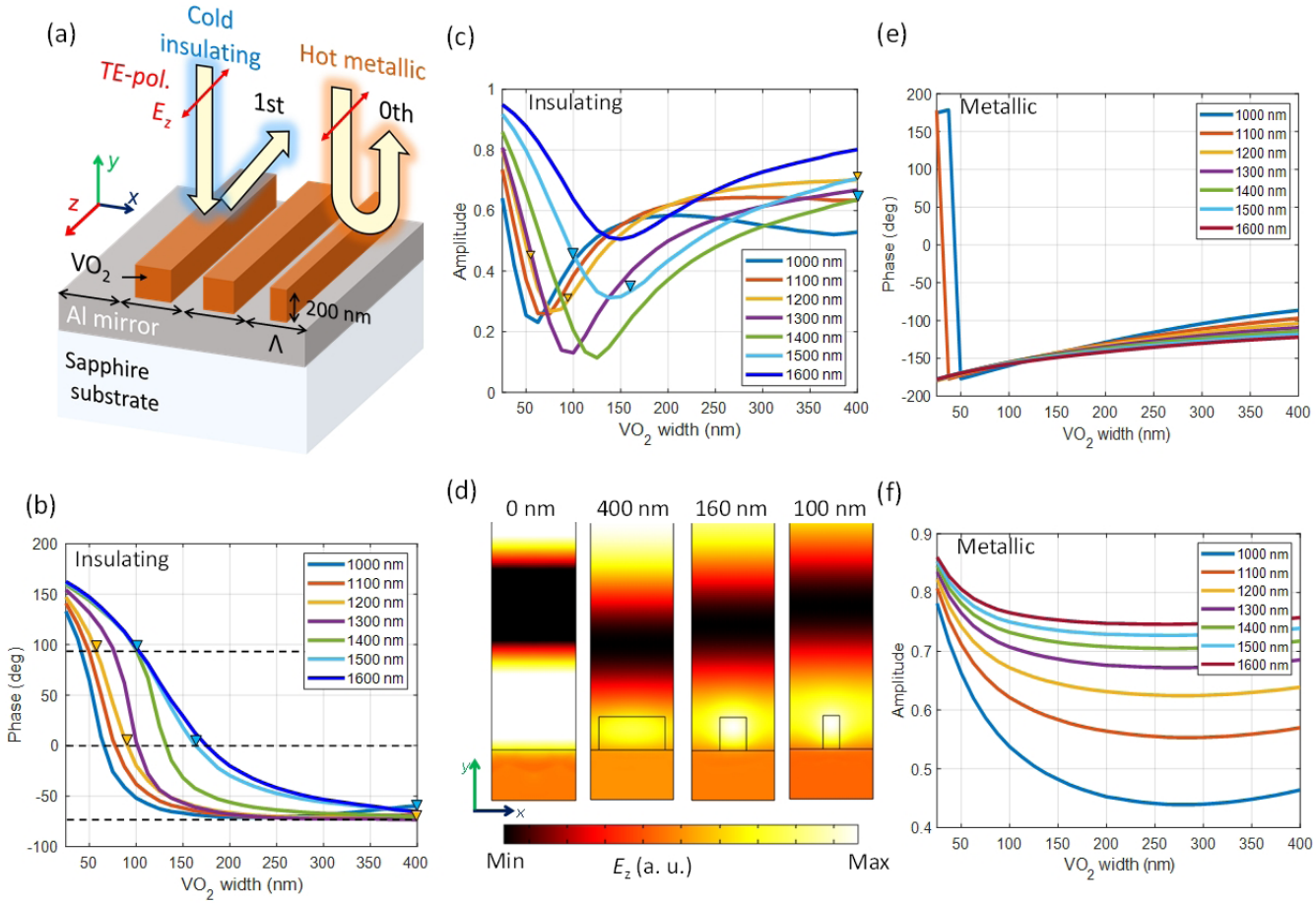

FIG. 2. Design of active beam deflector. (a) Schematic diagram of actively tunable beam deflector design. (b) Phase and (c) amplitude response of the VRW unit cell at the insulating phase according to the variation of VRW width and operation wavelength. (d) Normalized transvere electric field profiles of the insulating phase unit cells at the wavelength of 1500 nm. The VRW width are 0 nm, 400 nm, 160 nm, and 100 nm, from the left in order. (e) Phase and (f) amplitude response of the VRW unit cell at the metallic phase according to the variation of VRW width and operation wavelength.

beam switching device deflects normally incident TE light into the 1st and 0th orders, at the insulating and metallic phases, respectively.

The engineering of the device starts from numerical investigation of the unit cell characteristic, which determines the optical phase gradient of the supercell consisting of the four VRW unit cells. Even though the goal is to design optical reflection at both phases of the VRW metagrating, the proposed design only considers the insulating phase design for high performance operation, unlike other brute force optimization methods with heavy computation loads. Since interaction between TE light and VRW arrays would be negligible and would not differ significantly from the metallic mirror. The phase in Fig. 2(b) and amplitude in Fig. 2(c) of the unit cell reflection is numerically investigated at the insulating phase, according to variation of the VRW width and operation wavelength. Thickness and unit cell period (Λ) are fixed as 200 nm and 500 nm, respectively. Similar to conventional gradient metasurfaces, the optical phase gradient design is conducted based on generalized Snell's law for a one dimensional graded metagrating [2] as shown in Eq. (1) below. n_i, θ_i, θ_r, λ_i, and φ denote the refractive index of the incidence side, the incidence angle, the reflection angle, the incident wavelength, the phase profile on the metasurface, respectively:

$$n_i \sin\theta_r - n_i \sin\theta_i = \frac{\lambda_i}{2\pi}\frac{d\varphi}{dx}. \quad (1)$$

When seeing the amplitude plot in Fig. 2(c), a resonance dip occurs for narrow VRW widths depending on wavelength. To minimize amplitude modulation effect on reflection phase gradient, judicious selection of a center wavelength is necessary. The selection of VRW width values for supercell design, the widths for shifting 180, 90, 0, and –90 deg optical phase are required to build a supercell. For 180 deg phase shifting, no VRW structure is located on the Al mirror. Thus, the design issue is to choose proper width values for 90, 0, and –90 deg phase shifts with minimal amplitude modulation effect. Considering the aspects,

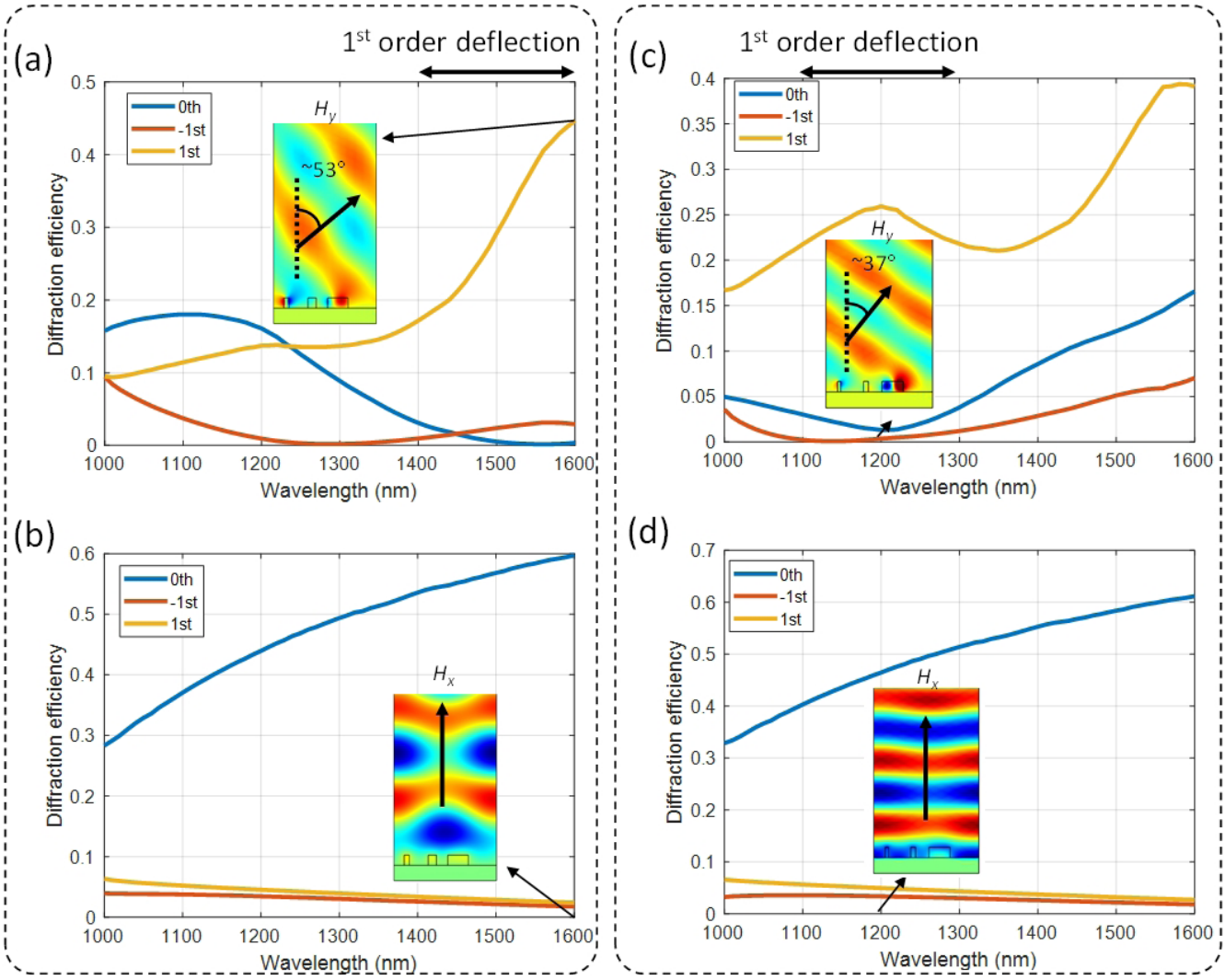

FIG. 3. Diffraction efficiency spectrum of the deflector design targeted for 1500 nm at the (a) insulating and (b) metallic phases, respectively. Diffraction efficiency spectrum of the deflector design targeted for 1200 nm at the (c) insulating, and (d) metallic phases, respectively. The inset figures denote normalized (a, c) vertical and (b, d) horizontal magnetic field profiles which describing reflection wavefront.

I chose width values for modulating reflection phase of 90, 0, and about –80 deg at the wavelength of 1200 nm and 1500 nm, respectively, for the two types of designs (See the dotted lines and inverted triangles of Figs. 2(b) and 2(c)). The width values for the 1200 nm design are 0 nm, 400 nm, 90 nm, and 60 nm, while those for 1500 nm are 0 nm, 400 nm, 160 nm, and 100 nm. The chosen unit cell responses at the insulating phase for 1500 nm design is graphically illustrated with normalized spatial profiles of the transverse electric field in Fig. 2(d). To check negligible modulation effects of phase and amplitude at the metallic VO_2 phase, the reflection coefficient is also numerically calculated at the metallic phase (Figs. 2(e) and 2(f)).

As shown in Figs. 3 and 4, the design performances of the two types of active beam deflectors turned out to be excellent in terms of signal efficiency, extinction ratio defined as R_1/R_0, and bandwidth. Here, R_0 and R_1 denote the zeroth and first order diffraction efficiency, respectively. The inset figures in Fig. 3 clearly verify high extinction ratio implying direction beam deflection characteristics and its thermal tunability. In the wavelength region around 1400–1600 nm, the type 1 device deflects incident light into the 1st order diffraction at the insulating phase, and switches the reflection direction to the 0th order when heated to the metallic phase (Figs. 3(a) and 3(b)). In case of the type 2 device, same function of active beam deflection occurs around the wavelength region of 1000–1300 nm (Figs. 3(c) and 3(d)). The deflection angle at the insulating phase toward the 1st order diffraction calculated from the following Eq. (2) ranges from 30 (at the wavelength of 1000 nm) to 53 (at the wavelength of 1600 nm) deg, where Λ refers to the supercell period which set to be 4 times the unit cell period:

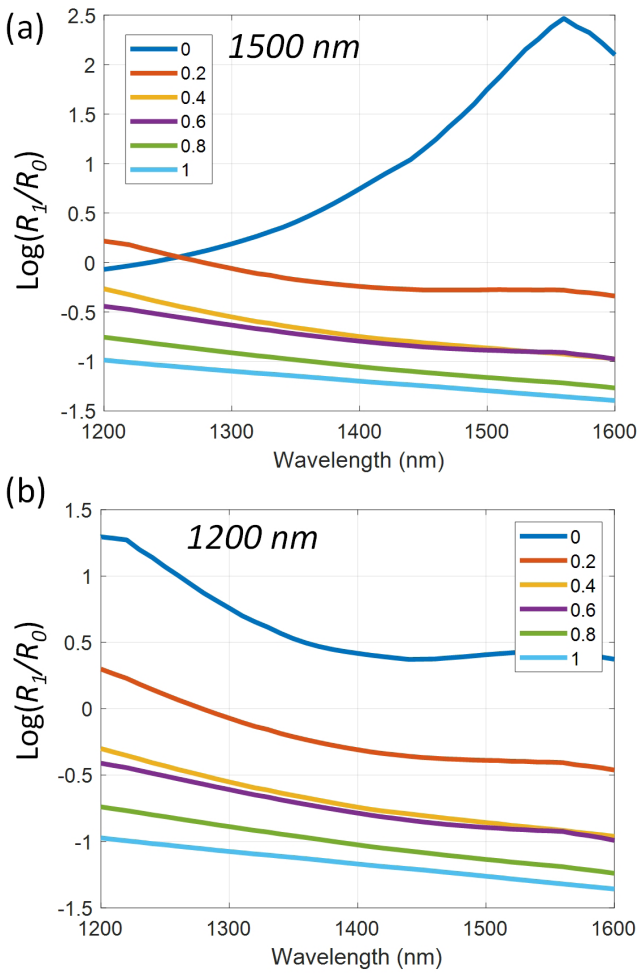

FIG. 4. Directional extinction ratio spectra according to the gradual phase change of VRWs. $\log_{10}(R_1/R_0)$ plots of the devices designed for (a) 1500 nm and (b) 1200 nm wavelength, respectively.

$$\theta_{+1} = \sin^{-1}\left(\frac{\lambda_1}{4\Lambda}\right). \quad (2)$$

Figures 3 and 4 suggest switchable power comparison between diffraction orders and the gradual phase change effect of VO_2 for both designs targeted around wavelengths of 1500 nm and 1200 nm. The gradual phase change effect of VO_2 is optically modelled as physical mixtures of the insulating and metallic phases according to Maxwell-Garnett effective medium theory [11]. The legends in Fig. 4 refer to fill factors of the metallic phase VO_2 so that increase of fill factor from 0 to 1 implies gradual phase change from insulating to metallic.

In addition, the abovementioned design can be extended to a tunable beam splitter under normal illumination and reflective operation as depicted in Fig. 5(a). The idea is to make a supercell with 7 discrete phase shifts by multiplexing increasing and decreasing sawtooth gradients in a single supercell. Thus, at the insulating phase, two types of gradients act as -1st and 1st order deflections while both

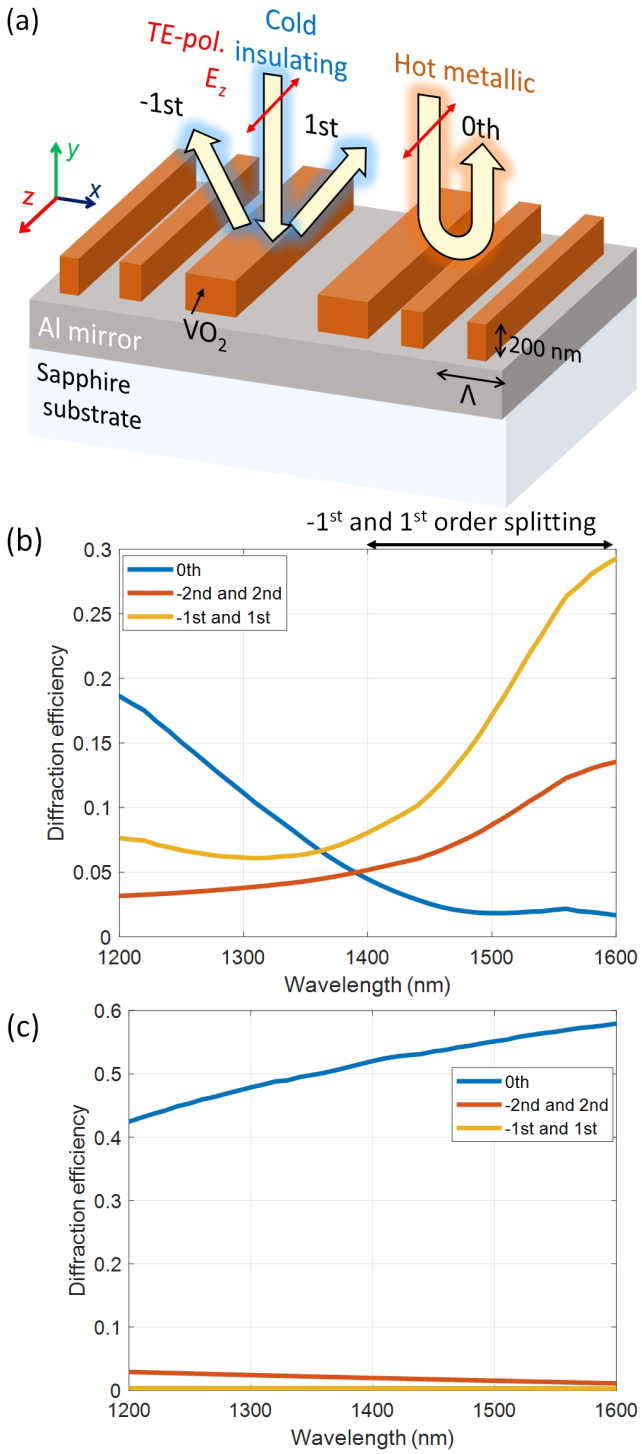

FIG. 5. Design of active beam splitter. (a) Schematic diagram of actively tunable beam splitter. Diffraction efficiency at the (b) insulating and (c) metallic phases, respectively. The legends in (b) and (c) denote the diffraction orders.

minimizing 0th order reflection (Fig. 5(b)). On the other hand, similar to the above designs, at the metallic phase, the device plays a mirror role by routing reflected light dominantly into the 0th order over broad bandwidth (Fig. 5(c)). I expect that further simultaneous numerical optimization

of thickness and widths of VRW, suppression of -2nd and 2nd order diffractions could be enhanced for increasing efficiency of the target beams.

III. CONCLUSION

In this paper, a novel reflective beam steering device design using nanostructured VO_2 metasurface grating is proposed for broadband efficient deflection and splitting with active thermal tunability. The electro-thermal modulation could also be possible when the metallic mirror is used as a Joule heating device with addressing of external electrodes. It is expected that the proposed design principles and ideas would be also fruitful for next-generation beam deflectors and spatial light modulators for modern digital holographic systems [30–32] for a wide range of applications.

ACKNOWLEDGMENT

This work was supported by 2020 Research Fund of Myongji University.

REFERENCES

1. N. Yu and F. Capasso, "Flat optics with designer metasurfaces," Nature Mater. **13**, 139–150 (2014).
2. N. Yu, P. Genevet, M. A. Kats, F. Aieta, J.-P. Tetienne, F. Capasso, and Z. Gaburro, "Light propagation with phase discontinuities: generalized laws of reflection and refraction," Science **334**, 333–337 (2011).
3. M. Khorasaninejad, W. T. Chen, R. C. Devlin, J. Oh, A. Y. Zhu, and F. Capasso, "Metalenses at visible wavelengths: diffraction-limited focusing and subwavelength resolution imaging," Science **352**, 1190–1194 (2016).
4. D. Lin, P. Fan, E. Hasman, and M. L. Brongersma, "Dielectric gradient metasurface optical elements," Science **345**, 298–302 (2014).
5. D. Lin, M. Melli, E. Poliakov, P. St. Hilaire, S. Dhuey, C. Peroz, S. Cabrini, M. Brongersma, and M. Klug, "Optical metasurfaces for high angle steering at visible wavelengths," Sci. Rep. **7**, 2286 (2017).
6. G. Zheng, H. Mühlenbernd, M. Kenney, G. Li, T. Zentgraf, and S. Zhang "Metasurface holograms reaching 80% efficiency," Nature Nanotechnol. **10**, 308–312 (2015).
7. H. Kim, "Metallic triangular pillar grating arrays for high transmission polarizers for air: glass interfaces," Jpn. J. Appl. Phys. **58**, 042001 (2019).
8. H. Kim, H. An, J. Kim, S. Lee, K. Park, S. Lee, S. Hong, L. A. Vazquez-Zuniga, S.-Y. Lee, B. Lee, and Y. Jeong, "Corrugation-assisted metal-coated angled fiber facet for wavelength-dependent off-axis directional beaming," Opt. Express **25**, 8366–8385 (2017).
9. C. Lei, Z. Man, and S. Tang, "Extraordinary optical transmission and enhanced magneto-optical Faraday effect in the cascaded double-fishnet structure with periodic rectangular apertures," Curr. Opt. Photon. **4**, 134–140 (2020).
10. J. W. Goodman, *Introduction to Fourier optics*, 3rd ed., (Roberts and Company Publishers, UK. 2005).
11. N. I. Zheludev and Y. S. Kivshar, "From metamaterials to metadevices," Nature Mater. **11**, 917–924 (2012).
12. S.-J. Kim, H. Yun, S. Choi, J.-G. Yun, K. Park, S. J. Jeong, S.-Y. Lee, Y. Lee, J. Sung, C. Choi, J. Hong, Y. W. Lee, and B. Lee, "Dynamic phase-change metafilm absorber for strong designer modulation of visible light," Nanophoton. **10**, 713–725 (2020).
13. S.-J. Kim, I. Kim, S. Choi, H. Yoon, C. Kim, Y. Lee, J. Son, Y. W. Lee, J. Rho, and B. Lee, "Reconfigurable all-dielectric Fano metasurfaces for strong intensity modulations of visible light," Nanoscale Horiz. **5**, 1088–1095 (2020).
14. S.-J. Kim, S. Choi, C. Choi, Y. Lee, J. Sung, H. Yun, J. Jeong, S.-E. Mun, Y. W. Lee, and B. Lee, "Broadband efficient modulation of light transmission with high contrast using reconfigurable VO_2 diffraction grating," Opt. Express **26**, 34641–34654 (2018).
15. S.-J. Kim, H. Yun, K. Park, J. Hong, J.-G. Yun, K. Lee, J. Kim, S. J. Jeong, S.-E. Mun, J. Sung, Y. W. Lee, and B. Lee, "Active directional switching of surface plasmon polaritons using a phase transition material," Sci. Rep. **7**, 43723 (2017).
16. M. J. Dicken, K. Aydin, I. M. Pryce, L. A. Sweatlock, E. M. Boyd, S. Walavalkar, J. Ma, and H. A. Atwater, "Frequency tunable near-infrared metamaterials based on VO_2 phase transition," Opt. Express **17**, 18330–18339 (2009).
17. Y. Kim, P. C. Wu, R. Sokhoyan, K. Mauser, R. Glaudell, G. K. Shirmanesh, and H. A. Atwater, "Phase modulation with electrically tunable vanadium dioxide phase-change metasurfaces," Nano Lett. **19**, 3961–3968 (2019).
18. C. Choi, S.-Y. Lee, S.-E. Mun, G.-Y. Lee, J. Sung, H. Yun, J.-H. Yang, H.-O. Kim, C.-Y. Hwang, and B. Lee, "Metasurface with nanostructured $Ge_2Sb_2Te_5$ as a platform for broadband-operating wavefront switch," Adv. Opt. Mater. **7**, 1900171 (2019).
19. Q. Wang, E. T. Rogers, B. Gholipour, C.-M. Wang, G. Yuan, J. Teng, and N. I. Zheludev, "Optically reconfigurable metasurfaces and photonic devices based on phase change materials," Nature Photon. **10**, 60–65 (2016).
20. H. D. Jeong and S. Y. Lee, "Tunable plasmonic absorber using a nanoslit array patterned on a $Ge_2Sb_2Te_5$-inserted Fabry–Pérot resonator," J. Lightwave Technol. **36**, 5857–5862 (2018).
21. J. Park, S. J. Kim, P. Landreman, and M. L. Brongersma, "An over-coupled phase-change metasurface for efficient reflection phase modulation," Adv. Opt. Mater. **8**, 2000745 (2020).
22. J. Park, J.-H. Kang, X. Liu, and M. L. Brongersma, "Electrically tunable epsilon-near-zero (ENZ) metafilm absorbers," Sci. Rep. **5**, 15754 (2015).
23. S. Kim, M. S. Jang, V. W. Brar, K. W. Mauser, L. Kim, and H. A. Atwater, "Electronically tunable perfect absorption in graphene," Nano Lett. **18**, 971–979 (2018).
24. M. M. Qazilbash, M. Brehm, B.-G. Chae, P.-C. Ho, G. O. Andreev, B.-J. Kim, S. J. Yun, A. V. Balatsky, M. B. Maple, F. Keilmann, H.-T. Kim, and D. N. Basov, "Mott transition in VO_2 revealed by infrared spectroscopy and nano-imaging," Science **318**, 1750–1753 (2007).
25. C. R. de Galarreta, A.M. Alexeev, Y.-Y. Au, M. Lopez-Garcia,

M. Klemm, M. Cryan, J. Bertolotti, and C. D. Wright, "Non-volatile reconfigurable phase-change metadevices for beam steering in the near infrared," Adv. Funct. Mater. **28**, 1704993 (2018).
26. A. Forouzmand and H. Mosallaei. "Dynamic beam control via Mie-resonance based phase-change metasurface: a theoretical investigation," Opt. Express **26**, 17948–17963 (2018).
27. T. Phan, D. Sell, E. W. Wang, S. Doshay, K. Edee, J. Yang, and J. A. Fan, "High-efficiency, large-area, topology-optimized metasurfaces," Light: Sci. Appl. **8**, 48 (2019).
28. H. Kim, J. Park, and B. Lee, *Fourier modal method and its applications in computational nanophotonics* (CRC Press, NY, USA. 2012).
29. P. B. Johnson and R. W. Christy, "Optical constants of transition metals: Ti, V, Cr, Mn, Fe, Co, Ni, and Pd," Phys. Rev. B **9**, 5056 (1974).
30. J. An, K. Won, Y. Kim, J.-Y. Hong, H. Kim, Y. Kim, H. Song, C. Choi, Y. Kim, J. Seo, A. Morozov, H. Park, S. Hong, S. Hwang, K. Kim, and H.-S. Lee, "Slim-panel holographic video display," Nature Commun. **11**, 5568 (2020).
31. Y. Kim, K. Won, Y. Kim, J. An, H. Song, S. Kim, C.-S. Choi, and H.-S. Lee, "Electrically tunable transmission-type beam deflector using liquid crystal with high angular resolution," Appl. Opt. **57**, 5090–5094 (2018).
32. C. Yoo, K. Bang, M. Chae, and B. Lee, "Extended-viewing-angle waveguide near-eye display with a polarization-dependent steering combiner," Opt. Lett. **45**, 2870–2873 (2020).